08,10

Electronic states genesis of the Ag_2Bi surface alloy on the Ag (4 2 3) vicinal surface

© Yu.M. Koroteev[1,2], D.V. Terenteva[3], L.A. Sviatkin[3], E.V. Chulkov[2]

[1] Institute of Strength Physics and Materials Science of the Siberian Branch of the Russian Academy of Sciences, Tomsk, Russia
[2] St. Petersburg State University, St. Petersburg, Russia
[3] National Research Tomsk Polytechnic University", Tomsk, Russia

E-mail: koroteev@ispms.tsc.ru

Received November 18, 2025
Revised December 1, 2025
Accepted December 8, 2025

To gain a deeper understanding of the band formation mechanism of the Ag_2Bi surface alloy on the Ag (4 2 3) vicinal surface, a first-principles study of its electronic structure is presented. The origin of the surface electronic states is investigated by tracing the evolution of the band structure upon transition from the smooth surface of the Ag_2Bi/Ag (1 1 1)-$(\sqrt{3}\times\sqrt{3})R\,30^\circ$) system to the Ag_2Bi/Ag (4 2 3) vicinal surface, as well as upon transition from the flat configuration $(2\sqrt{3}\times\sqrt{3})R\,30^\circ$ of a free-standing monolayer of the Ag_2Bi surface alloy to the (4 2 3) vicinal configuration, and further to ultrathin Ag films with a thickness of 1 and 3 monolayers, on one side of which the Ag_2Bi surface alloy is located. The role of the stepped nature of the surface, silver atoms of the substrate, and Bi atoms relaxation in shaping the electronic spectrum of the Ag_2Bi surface alloy on the Ag (4 2 3) vicinal surface is discussed.

Keywords: spin-orbit interaction, electronic structure, surface states, Bychkov−Rashba effect.

DOI: 10.61011/PSS.2026.01.63251.8793-25

1. Introduction

The giant spin-orbit splitting of the electronic states of the Ag_2Bi/Ag (1 1 1) surface alloy discovered in 2007 [1,2] has aroused great interest in systems of this type, and the surface alloy itself Ag_2Bi has been the subject of numerous experimental and theoretical studies, as well as review papers [3–11], devoted to the study of the features of its atomic and electronic structure, spin and orbital texture. It was concluded in Refs. [1,2] that the giant spin splitting in the Ag_2Bi/Ag (1 1 1) surface alloy is the result of a large potential gradient in the surface plane resulting from a violation of the inversion symmetry of the surface layer and significant outward relaxation of Bi atoms. In the electron's rest system, this gradient manifests itself as an effective magnetic field along the normal to the surface, which leads to increased spin splitting and the appearance of nonzero z components of spin polarization. Calculations for a two-dimensional electron gas model that goes beyond the standard Bychkov−Rashba scheme performed in Ref. [3] fully confirmed these conclusions.

To study the mechanism of giant spin splitting of the Bychkov−Rashba type, a low-energy electron diffraction method was used in [5], which allowed find a outward relaxation of surface alloy atoms. The authors concluded that the atomic structure of the surface alloy plays an important role in spin splitting, since it determines the potential relief and significantly affects the overlap of atomic orbitals and, as a result, the dispersion of electronic energy bands. The atomic structures that occur during deposition of Bi onto the Ag (1 1 1) surface depending on the degree of coverage were studied in Ref. [6]. It was found that with a low degree of coating, Bi atoms form a Ag_2Bi surface alloy in the $(\sqrt{3}\times\sqrt{3})R\,30^\circ$ structure, which, when coated above 0.55 of the monolayer, transforms into an ordered rectangular structure $(p\times\sqrt{3})$ of a Bi atoms layer on the Ag (1 1 1) surface.

To explain the anisotropy of the Bychkov−Rashba effect observed in the electronic spectrum of the Ag_2Bi/Ag (1 1 1)-$(\sqrt{3}\times\sqrt{3})R\,30^\circ$ surface alloy, the authors of Ref. [7] using the $\mathbf{k}\cdot\mathbf{p}$-method of the theory of perturbations involving spin-orbit interaction built effective Bychkov−Rashba Hamiltonians for various point groups, up to the third order in a wave vector. A comparison of the results obtained with the data from relativistic *ab initio* calculations allowed the authors to clearly identify the contributions and influence of the corresponding 3rd order Rashba parameters and establish that the isotropic and anisotropic contributions are related to the gradients of the crystal potential normal to the surface and in the surface plane, respectively

Investigation of electron scattering by atomic steps of a Ag_2Bi monolayer on an Ag (1 1 1) surface using measurements of the quasiparticles interference and calculations of

the spin and orbital textures of the electronic states of this monolayer in the framework of density functional theory (DFT) [8] revealed the spin-flip backscattering mechanism that is not predicted by Bychkov–Rasba's theory of surface states. Due to the different degrees of localization of occupied and unoccupied electronic states of Ag and Bi, this mechanism is very sensitive to the chemical composition of the edges of the steps.

The combined effect of exchange and spin-orbit interactions on the surface states and quantum well states of Ag_2Bi/Ag films grown on ferromagnetic Fe (1 1 0) was studied in Ref. [9]. As shown by photoemission studies and *ab initio* calculations, the concurrent breaking of time-reversal and translational symmetry led to spin-selective hybridization of Bychkov–Rashba surface states with quantum well states split by exchange interaction. As a result, asymmetric and spin-dependent forbidden slits were found, an inequality in the number of states appeared along the opposite directions of the Brillouin zone ($\mathbf{k}$ and $-\mathbf{k}$), and arc-shaped contours of constant energy appeared. It has been suggested that the resulting asymmetry of the electronic structure can significantly affect the properties of spin-polarized transport.

A significant rearrangement of the electronic spectrum of the Ag_2Bi surface alloy was also noted in our recent paper Ref. [12] on vicinal surfaces of Ag (4 2 3) and Ag (11 7 9), where the translational symmetry of the crystal is violated not only by the surface, but also by arrays of steps on it. Using curved Ag crystals to select local vicinal planes, we found two „magic" (especially stable) vicinal surfaces with lattices of atomically sharp straight (without kinks) steps, stabilized by the Ag_2Bi surface alloy. Angular-resolution photoemission experiments, as well as calculations of electronic states using the DFT approach, have shown that the scattering of Bychkov–Rashba surface states (i. e. split by spin-orbit interaction) on the steps of the vicinal surfaces (4 2 3) and (11 7 9) leads to an orbitally selective renormalization of the zones in the direction perpendicular to the steps and deep modulation. planar orbital dichroism. The effect of strong repulsive scattering on the steps was observed mainly for the p_y-type bands. It is shown that the interaction of Bychkov–Rashba electrons with a steps superlattice of vicinal surface leads to a strong change in the spin texture, removing the spin from the initial spiral configuration in the plane.

Despite a rather detailed discussion in Ref. [12] of the electronic structure and spin texture of the Ag_2Bi surface alloy on the vicinal surfaces of Ag (4 2 3) and Ag (11 7 9), there are still a number of unresolved issues. In particular, it was noted that the complex orbital-selective renormalization of the bands of the Ag_2Bi surface alloy found in the study is far from the picture of the reverse folding of rigid bands In addition, the question of the origin of the non-coplanar spin textures of the Ag_2Bi surface alloy on the (4 2 3) and (11 7 9) vicinal surfaces remained unanswered.

Therefore, the purpose of this work is an *ab initio* study the electronic structure of the Ag_2Bi surface alloy on the vicinal surface of Ag (4 2 3), to establishe the role of the stepwise (vicinal) character of the surfce, the roles of Ag substrate atoms and the Bi atoms relaxation in the formation of a surface alloy electronic spectrum

2. Calculation method and details

The electronic structure of the Ag_2Bi surface alloy on the smooth Ag (1 1 1)-$(\sqrt{3}\times\sqrt{3})R\,30^\circ$ and vicinal Ag (4 2 3) surfaces was calculated. The electronic structure of the Ag_2Bi surface alloy on the smooth Ag (1 1 1)-$(\sqrt{3}\times\sqrt{3})R\,30^\circ$ and vicinal Ag (4 2 3) surfaces was calculated. The electronic spectrum of the surface (1 1 1) was also calculated with a $(2\sqrt{3}\times\sqrt{3})R\,30^\circ$ calculation cell to study the genesis of the surface states observed in the experiment and DFT calculations on the (4 2 3) vicinal surface in Ref. [12]. The surface layer of this calculation cell had almost the same atomic structure and contained exactly the same number of Bi and Ag atoms as the terrace of the (4 2 3) vicinal surface. The atomic structures of the surfaces mentioned above are shown in Figure1, which shows that there are 4 Ag atoms and 2 Bi atoms in the upper layer of the unite cell of the (4 2 3) film. The Bi atoms are arranged in such a way that one of them lies on the terrace, and the other forms the edge of the step.

The (1 1 1) smooth and (4 2 3) vicinal silver surfaces on which the Ag_2Bi surface alloy was located were modeled with asymmetric films of 21 (thickness ~ 65 Å) and 28 (thickness ~ 70 Å) atomic layers, respectively. Moreover, the genesis of the surface states observed in Ref. [12] was studied by calculating the electronic structure of hypothetical free-standing monolayers of the Ag_2Bi surface alloy in the $(2\sqrt{3}\times\sqrt{3})R\,30^\circ$ structure of a (1 1 1) smooth surface and in the structure of the (4 2 3) vicinal surface, as well as the Ag_2Bi surface alloy on ultrathin Ag films with a thickness of 1 and 3 monolayers. The role of relaxation of the atomic structure (positions of Bi atoms) of monolayers of the Ag_2Bi surface alloy in planar $(2\sqrt{3}\times\sqrt{3})R\,30^\circ$ and vicinal configurations was determined by calculating their electronic structure for three positions of Bi atoms: (i) Bi atoms are located in a layer of atoms Ag (nonrelaxed monolayer); (ii) Bi atoms are displaced along the axis Z (in the vacuum direction) by 1/2 of the relaxed position, and (iii) Bi atoms are in a completely relaxed position The fully relaxed position refers to the position of Bi atoms (i. e., as on the surface of thick relaxed films — smooth and vicinal).

We optimized the positions of the atoms in the four surface layers of the films and observed significant external relaxation of the Bi atoms. It was 0.75 Å on the (1 1 1) smooth surface, and it was 0.67 Å on the (4 2 3) vicinal surface for Bi atoms on the terrace and 0.13 Å for Bi atoms forming the edge of the step. In both cases, the Bi atoms are displaced almost perpendicular to the plane of the terrace. Experimental measurements of low-energy electron diffraction (LEED) [5] on the (1 1 1) smooth surface yielded the value of the external relaxation 0.65 ± 0.10 Å, and the

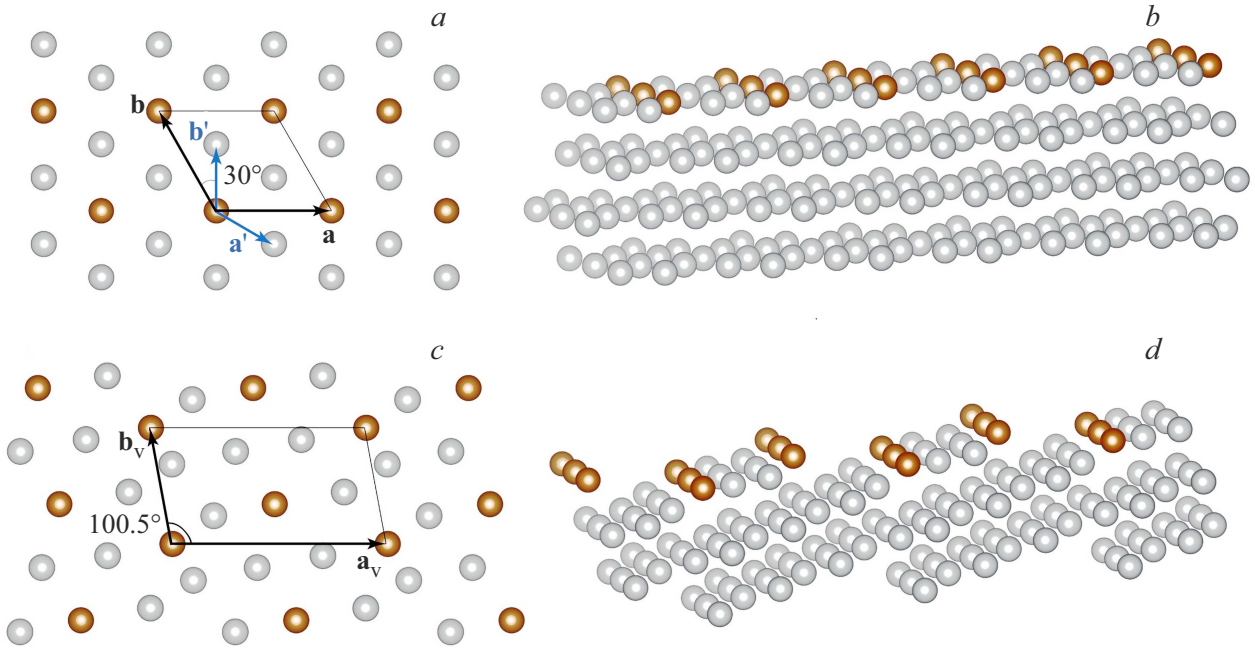

Figure 1. Atomic structure of the Ag_2Bi surface alloy on the smooth Ag (1 1 1)-$(\sqrt{3}\times\sqrt{3})R\,30^\circ$ (a, b) and vicinal Ag (4 2 3) (c, d) surfaces. Top view (a, c) and side view (b, d) (it shown the upper and several subsurface layers only). $\mathbf{a}'$ and $\mathbf{b}'$ — lattice vectors of the Ag (1 1 1) surface. bf a, b — lattice vectors of the $(\sqrt{3}\times\sqrt{3})R\,30^\circ$ structure. The modules of these vectors are related by the ratio $|\mathbf{a}| = |\sqrt{3}\mathbf{a}'|$, $|\mathbf{b}| = |\sqrt{3}\mathbf{b}'|$. $\mathbf{a}_v$, $\mathbf{b}_v$ — lattice vectors of the vicinal surface Ag (4 2 3). The gray balls represent Ag atoms, the orange balls represent Bi atoms.

calculations *ab initio* yielded 0.35 Å [1] and 0.85 Å [2], which agrees well with our results.

All calculations were performed within the framework of the DFT approach using the projector augmented wave (PAW) method [13] implemented in the VASP code [14,15]. The exchange-correlation potential was taken into account in the approximation of a generalized gradient in the Purdue–Burke–Ernzerhof form [16]. Scalar-relativistic corrections were included in the Hamiltonian, and the spin-orbit interaction was taken into account by the method of the second variation [17]. The calculations used a basic set of plane waves with energy up to 250 eV. The electronic structure of the surface was calculated using a repeating film model. The Brillouin zone integration was performed using Gaussians with the „smearing" parameter 0.01 eV. Self-consistensy of the electron density was carried out with an accuracy of 10^{-5} eV/atom. At each iteration of the self-consistency, the eigenvalues of the Hamiltonian were calculated on grids of k-points $(5\times5\times1)$ and $(3\times5\times1)$ in the whole Brillouin zone for the smooth $(\sqrt{3}\times\sqrt{3})R\,30^\circ$, as well as smooth $(2\sqrt{3}\times\sqrt{3})R\,30^\circ$ and vicinal Ag (4 2 3) surfaces, respectively. The atomic structure relaxation of the films surfaces was carried out up to the 8th layer and was carried out until the forces acting on the atoms became less than 10 meV/Å. The sites of the atoms in the remaining part of the films were fixed as in an ideal face-centered cubic lattice. The vacuum layer thickness for all calculations was $\sim$ 12 Å.

3. Results and discussion

3.1. Electronic structure of thick films

Figure 2 shows the calculation cells and the corresponding Brillouin zones with indication $k$points of high symmetry, as well as the electron-energy band structures of the Ag_2Bi surface alloy on the smooth (1 1 1) and vicinal (4 2 3) surfaces of silver. In the coordinate system we have chosen, the steps of the (4 2 3) vicinal surface are located perpendicular to the x axis, i.e., the two-dimensional lattice vector $\mathbf{a}$ is directed at a small angle ($\sim 10.5^\circ$) to the step. The D_{xy} orbital dichroism was calculated to analyze the orbital composition of surface states using the formula $D_{xy} = (p_x - p_y)/(p_x + p_y)$, where p_x and p_y are the contributions of the corresponding Bi p-orbitals. In Figure 2, c, the blue circles correspond to the condition $D_{xy} > 0$, which means the predominance of the p_x-orbitals contribution , and the red circles correspond to the condition $D_{xy} < 0$, which corresponds to the predominance of the p_y-orbitals contribution. The contributions of the Bi p_z-orbitals hybridized with the Ag s-orbitals are not shown, since they are dominant only in the upper part of the Bychkov–Rashba parabolas s_1 (above the Kramers degeneracy point), i.e., in a very small part of the Brillouin zone (see Figure S5 and S6 in Ref. [18]).

Let us consider the evolution of the electronic structure of the Ag_2Bi surface alloy during the transition from the Ag (1 1 1) smooth surface to the (4 2 3) vicinal one.

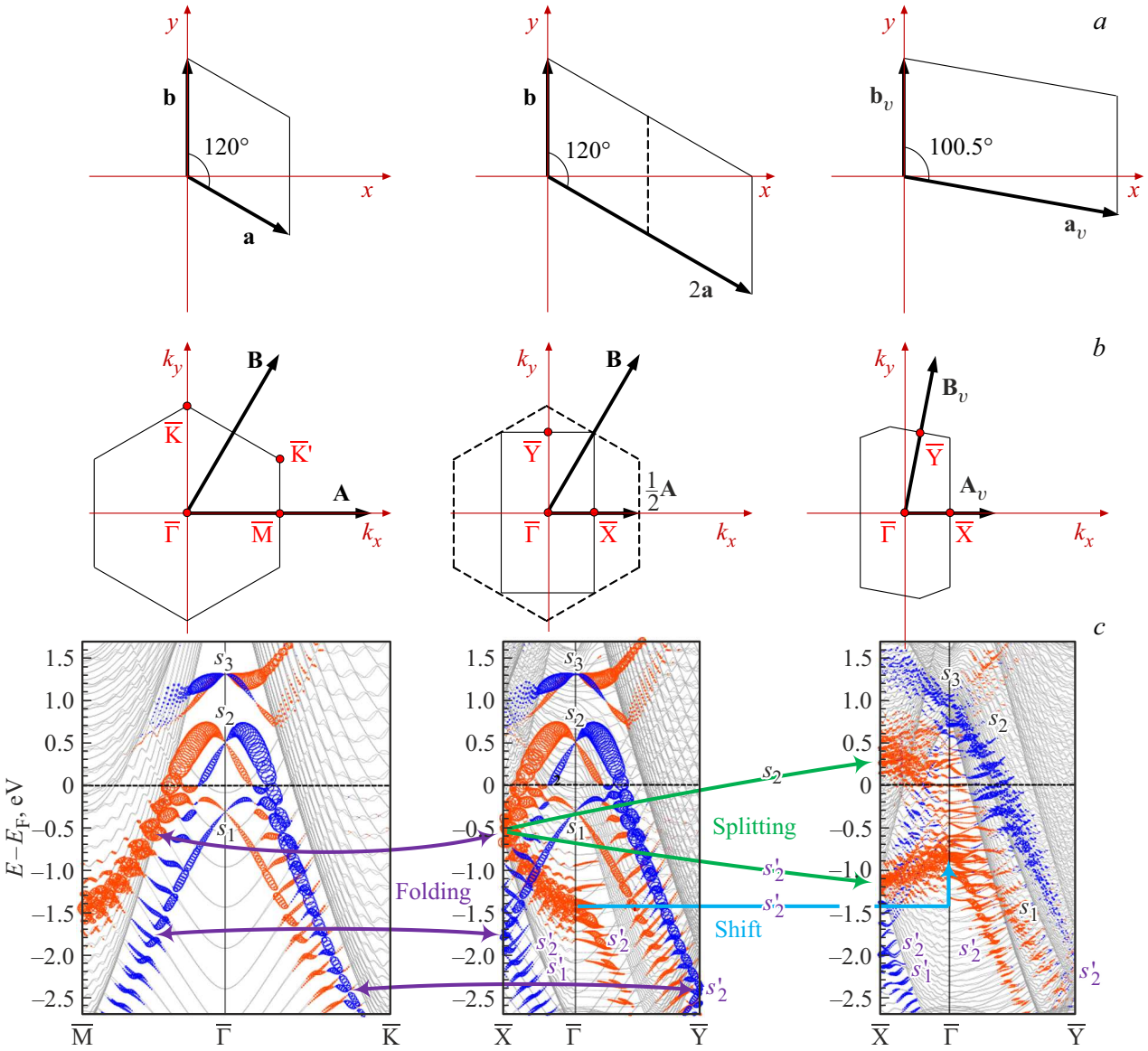

Figure 2. *a*) Unit cells and lattice vectors, *b*) Brillouin zones, reciprocal lattice vectors and high symmetry points, *c*) electronic band spectrum of the Ag_2Bi surface alloy on the smooth surface Ag (1 1 1) in the structures $(\sqrt{3}\times\sqrt{3})R\,30°$ (left), $(2\sqrt{3}\times\sqrt{3})R\,30°$ (center) and on the Ag (4 2 3) vicinal surface (on the right). The bands with a large contribution of Bi p_{xy}-states are shown by their orbital dichroism D_{xy} in blue ($D_{xy} < 0$) and red ($D_{xy} > 0$) circles. The radii of the circles are proportional to the magnitude of the orbital dichroism D_{xy}. The light gray lines show the energy bands of the silver substrate.

The electronic spectra shown in Figure 2, *c* demonstrate the strong and complex influence of surface vicinality on the dispersion dependence $E(\mathbf{k})$ of Bychkov–Rashba spiral states of the $Ag_2B/Ag\,(1\,1\,1)$-$(\sqrt{3}\times\sqrt{3})R\,30°$ smooth surface, marked with the s_1, s_2 and s_3 letters. The influence of vicinality is determined by two factors: the size effect (the unit cell of the (4 2 3) vicinal surface contains twice as many atoms as the unit cell of the $(\sqrt{3}\times\sqrt{3})R\,30°$ smooth surface) and the influence of a step potential on the surface. To analyze the size effect, we calculated the electronic structure of the $Ag_2Bi/Ag\,(1\,1\,1)$ smooth surface in the $(2\sqrt{3}\times\sqrt{3})R\,30°$ structure, that is, with a surface unit cell doubled along one of the lattice vectors Since the atom sites in the $(2\sqrt{3}\times\sqrt{3})R\,30°$ unit cell almost coincides with the atom sites on the terrace of the vicinal surface, a comparison of the electronic spectra of this smooth surface and the (4 2 3) vicinal surface allowed revealing the step potential effect on the electronic spectrum of the Ag_2Bi surface alloy.

The left panel of Figure 2, *c* shows the calculated spectrum of the $Ag_2B/Ag\,(1\,1\,1)$-$(\sqrt{3}\times\sqrt{3})R\,30°$ smooth surface. $Ag_2B/Ag\,(1\,1\,1)$-$(\sqrt{3}\times\sqrt{3})R\,30°$, It agrees very well with the results of calculations by other authors [2]. The central panel of Figure 2, *c* shows the electronic spectrum of the $(2\sqrt{3}\times\sqrt{3})R\,30°$ smooth surface. The violet arrows show the result of folding the $\overline{\mathrm{M\Gamma}}$ and $\overline{\Gamma\mathrm{K}}$ directions of the

hexagonal Brillouin zone of the $(\sqrt{3}\times\sqrt{3})R\,30^\circ$ structure into the $\overline{\Gamma X}$ and $\overline{\Gamma Y}$ directions, respectively, of the rectangular Brillouin zone of the $(2\sqrt{3}\times\sqrt{3})R\,30^\circ$ structure. It is clearly seen that the left branches of the Bychkov–Rashba states propagating from $\overline{\Gamma}$ point to $\overline{M}$ point downwards in energy, in the middle of the $\overline{M\Gamma}$ direction corresponding to the $\overline{X}$ point of the rectangular Brillouin zone of the $(2\sqrt{3}\times\sqrt{3})R\,30^\circ$ structure, are reflected from the boundary of the rectangular Brillouin zone and propagate back to the $\overline{\Gamma}$ point. Folding of the hexagonal Brillouin zone into the rectangular one reduces the $\overline{\Gamma K}$ direction to the $\overline{\Gamma Y}$ direction (see the central panel of Figure 2, *b*). This leads to the reflection of four Bychkov–Rashba states from the boundary of the new Brillouin zone, propagating downwards in energy from the $\overline{\Gamma}$ point to the $\overline{K}$ point. In addition, a band is observed in the spectrum of the $(2\sqrt{3}\times\sqrt{3})R\,30^\circ$ surface in the $\overline{\Gamma Y}$ direction, at energies below -1.4 eV, resulting from the folding of the $\overline{MK'}$ and $\overline{\Gamma K}$ directions of the hexagonal Brillouin zone of the $(\sqrt{3}\times\sqrt{3})R\,30^\circ$ surface. Thus, we have described a modification of the spectrum of the $(\sqrt{3}\times\sqrt{3})R\,30^\circ$ smooth surface due to doubling its unit cell along one of the lattice vectors.

Let us consider a modification of the Bychkov–Rashba states spectrum of the $(2\sqrt{3}\times\sqrt{3})R\,30^\circ$ smooth surface at the transition to the (4 2 3) vicinal surface, that is, when a monatomic steps lattice appears. As can be seen from Figure 2, *a* and *b*, the unit cells and Brillouin zones of the $(2\sqrt{3}\times\sqrt{3})R\,30^\circ$ smooth and (4 2 3) vicinal surfaces have approximately the same size and slightly different shape. The steps of the (4 2 3) vicinal surfaceare oriented perpendicular to the *X* axis, therefore, as can be seen from the left panel of Figure 2, *b*, the $\overline{\Gamma X}$ symmetrical direction is perpendicular to the step. In this case, the $\mathbf{k}_y$ vector is not parallel to the step, therefore the $\overline{\Gamma Y}$ symmetrical direction of the Brillouin zone of the vicinal surface lies at a slight angle ($\sim 10.5^\circ$) to it. It should be noted that in the case of the smooth surface (the middle panel of Figure 2, *b*), the $\overline{\Gamma Y}$ symmetrical direction is perpendicular to the *X* axis, that is, the $\overline{\Gamma Y}$ directions do not coincide on the smooth and vicinal surfaces, but they lie at the small angle to each other.

The light blue and green arrows in Figure 2, *c* show the result of the action of the step potential of the (4 2 3) vicinal surface. It can be seen that the scattering of the Bychkov–Rashba states of the smooth surface at the steps of the vicinal surface leads to a drastic change in the bands dispersion formed mainly by the p_y-orbitals, whereas the p_x state bands are not modified so much. The greatest changes of the bands dispersion are observed along the $\overline{X\Gamma}$ direction perpendicular to the steps. Namely, the s_2 band on the (1 1 1) smooth surface, formed predominately by the p_y-states, foldeed at the $\overline{X}$ point (s_2 and s_2' bands), on the (4 2 3) vicinal surface splits at the $\overline{X}$ point by about 1.5 eV as a result of the scattering on the steps, and changes its dispersion along the $\overline{X\Gamma}$ direction. On the contrary, on the (1 1 1) smooth surface the s_1 and s_2 bands formed mostly by the p_x-states, that also folded at

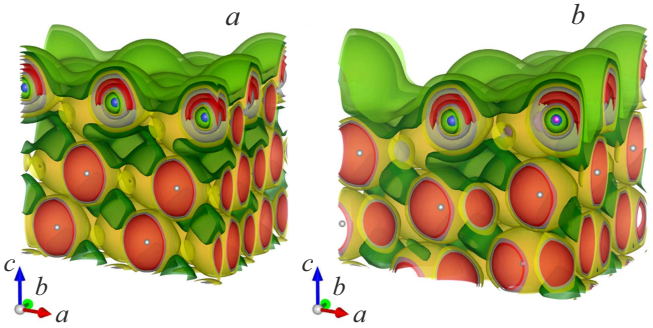

Figure 3. Distribution of the electron density of the Ag_2Bi surface alloy *a*) on the Ag (1 1 1) smooth surface and *b*) on the Ag (4 2 3) vicinal surface. The position of the Ag(Bi) atoms is shown by small light gray (purple) balls. The light green isosurfaces correspond to the electron density 0.01 e/Å^3, dark green — 0.02 e/Å^3, yellow — 0.03 e/Å^3, gray — 0.04 e/Å^3, red — 0.05 e/Å^3.

the $\overline{X}$ point, practically do not change their dispersion on the vicinal surface, only becoming more diffuse (blurred) due to scattering on the steps of the vicinal surface, and therefore appearing less clearly in Figure 2, *c*.

We do not discuss here the contribution of the p_z-orbitals of Bi, because the step potential of the vicinal surface blur its contributions acoss a large number of bands. As a result, there are no bands with a predominant contribution of Bi p_z-orbital on the (4 2 3) vicinal surface. The corresponding illustration can be seen in Figure S6 in Ref. [18].

Figure 3 shows the electron density distributions of their Ag_2Bi surface alloy on the (1 1 1) smooth and (4 2 3) vicinalsilver surfaces. The large anisotropy of the valence charge distribution on the Bi atoms of the surface alloy is clearly visible. The dipole moment of Bi atoms on the terrace of the (4 2 3) vicinal surface is directed almost orthogonally to the terrace, i.e. as on the (1 1 1) smooth surface. It can be seen from Figure 3, *b* that the dipole moment of the Bi atoms forming the step edge is oriented approximately at an angle of 45° to the terrace plane.

The difference in the Bi atoms binding located at the step edge and on the terrace with their nearest neighbors leads to different directions of these atoms polarization due to the anisotropic valence charge distribution, which is clearly seen in Figure 3 As a result, a potential gradient appears on the vicinal surface, and hence an electric field with in-plane and out-of-plane components, which, acting on electrons in surface bonds, lead to different orientations of spin polarization.

3.2. Electronic structure of monolayers and ultrathin films

Figure 4 shows the electron band spectra of the free-standing monolayers of the Ag_2Bi surface alloy in the $(2\sqrt{3}\times\sqrt{3})R\,30^\circ$ structure of the (1 1 1) smooth and (4 2 3) vicinal surfaces calculated for the three posi-

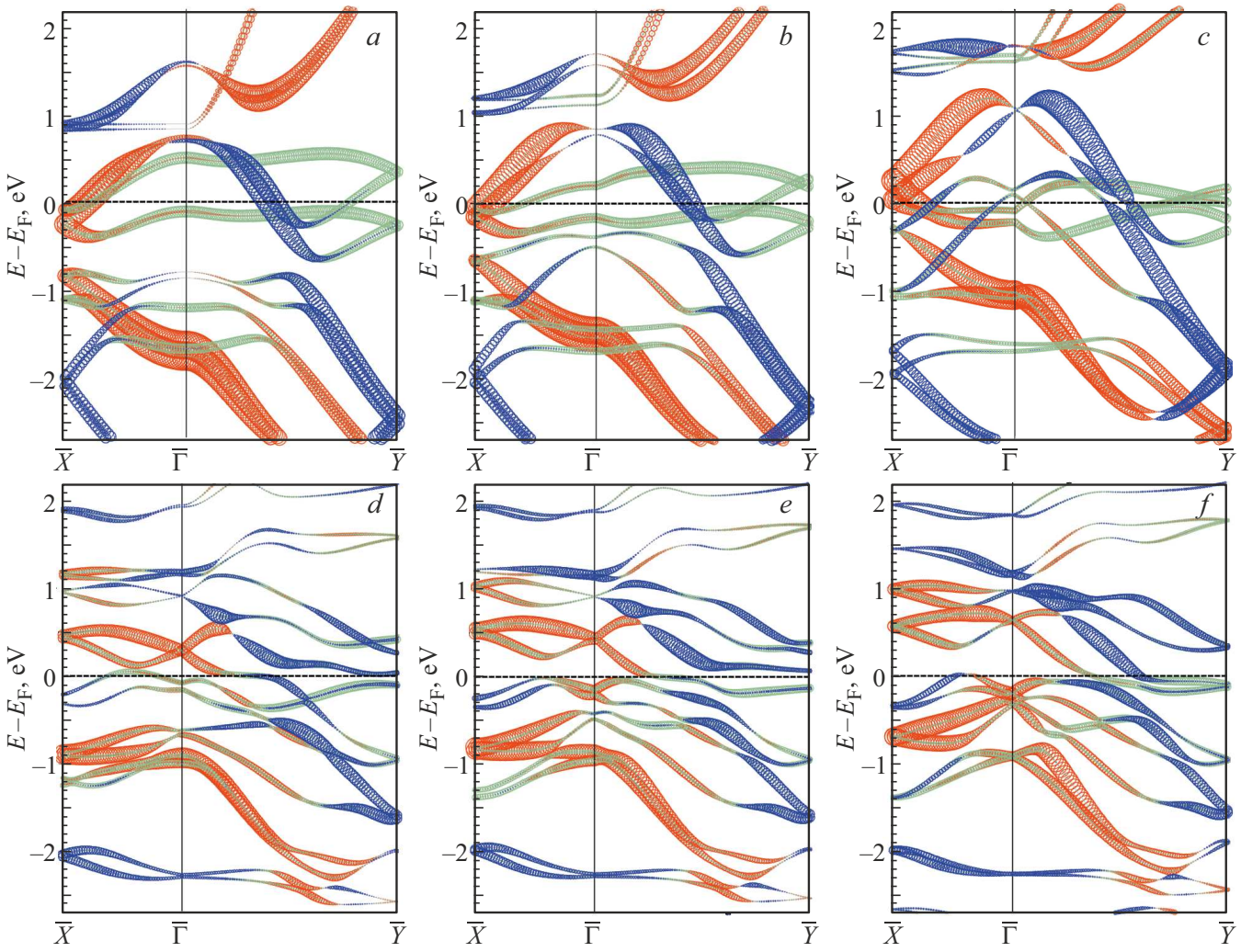

Figure 4. Electronic band spectra of the free-standing hypothetical monolayers of the Ag_2Bi surface alloy in the $(2\sqrt{3}\times\sqrt{3})R\,30°$ structure of the (1 1 1) smooth surface (a–c) and in the structure of the (4 2 3) vicinal surface (d–f) calculated for three positions of the Bi atoms: a, d) the Bi atoms are located in the Ag atoms layer (an unrelaxed monolayer); b, e) the Bi atoms are shifted along the Z axis (in the vacuum direction) by 1/2 of the relaxed position, and c, f) the Bi atoms are in the completely relaxed position. The bands with a large contribution of the Bi p_{xy}-states are shown with their orbital dichroism D_{xy} by blue ($D_{xy} < 0$) and red ($D_{xy} > 0$) circles. The contribution of the p_z-orbitals is shown by green circles. The radii of the circles are proportional to the magnitude of the D_{xy} orbital dichroism and the contribution of the p_z-orbitals.

tions of Bi atoms. As seen in Figure 4, a–c, the displacement of Bi atoms from the Ag atoms layer leads to a significant transformation of the monolayer electronic spectrum of the Ag_2Bi surface alloy of the planar configuration. This is due both to a change (weakening) of the hybridization of the Ag and Bi atoms electronic states, and to the manifestation of a spin-orbit interaction of the Bychkov–Rashba type attributable to the appearance of a surface potential gradient $\partial V/\partial z$ along the normal to the surface. The p_z-type states undergo a significant transformation, their contribution decreases with increasing the Bi atoms displacement. In addition, this displacement leads to an increase in the absolute value of the $|D_{xy}|$ orbital dichroism (i. e., to a clearer separation of the contributions of p_x- and p_y-type states) as a result of the formation of two complexes bands of the Bychkov–Rashba type in the energy range of 0.1 and 1.1 eV in Figure 4, c (bands marked in blue and red). As can be see on Figure 4, a–c that these complexes arise as a result of the transformation of two pairs of bands at energies −0.85 and 0.7 eV at the $\overline{\Gamma}$ point in Figure 4, a. With an increase in the Bi atoms displacement, the bands formed by the Bi p_x- and p_y-states tend to lower binding energies (shift upward in energy), and the bands formed with the participation of the Bi p_z-states shift to higher binding energies.

Before analyzing the electronic spectra of the vicinal configuration of the Ag_2Bi surface alloy monolayer (Figure 4, d–f), we make the following remark. As we have already reported, the Bi atoms forming the edge of the step on the surface of a thick film (4 2 3) are

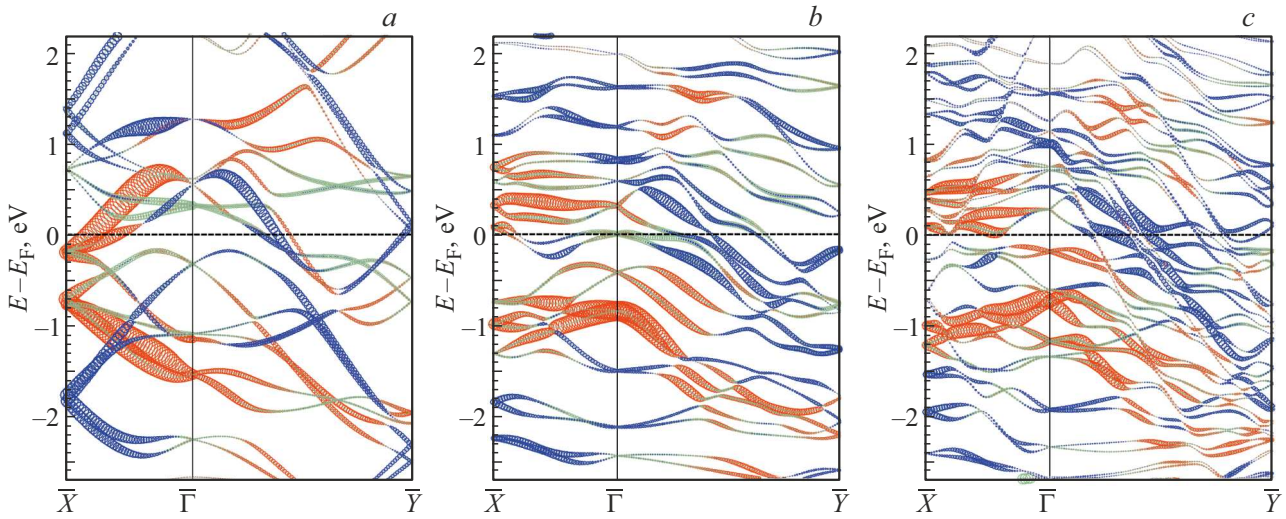

Figure 5. Electronic band spectra of the Ag_2Bi monolayers in *a*) the (1 1 1)-$(2\sqrt{3}\times\sqrt{3})R\,30^\circ$ flat and *b, c*) (4 2 3) vicinal configurations on the substrates consisting of the one (a, b) and three (c) layers of silver. The red and blue circles show the D_{xy} orbital dichroism of bands, the green circles show the p_z-states contribution . The radii of the circles are proportional to the magnitude of the represented characteristic.

displaced by relaxation from the terrace plane much weaker (more than five times) than the Bi atoms on the terrace. Therefore, we did not displace these atoms in the electronic structure calculations of the monolayer. Thus, the transition from Figure 4, *d* to Figure 4, *f* shows only the relaxation effect of atomic positions on the terrace, and the transition from Figure 4, $a-c$ to Figure 4, $d-f$ — the influence of vicinality on the electronic spectrum of a hypothetical monolayer. Therefore, the bands experiencing the greatest changes during the transition from Figure 4, *d* to Figure 4, *f*, should be associated with Bi atoms on the terrace (because they experience displacement), and the bands that almost do not change their position and shape should be associated with Bi atoms forming the edge of the step, because they are did not shift in the calculations.

Analysis of the electronic spectra of the Ag_2Bi surface alloy monolayer in the vicinal configuration ((Figure 4, $d-f$) revealed that displacement of Bi atoms from the terrace plane leads to a significant transformation of these spectra. However, in this case, there is no reduction of the Bi p_z-type states contribution, as was observed for the smooth monolayer, but a significant decrease in their contribution is observed compared to the smooth monolayer (the latter effect is the influebce of the vicinality).

Considering in pairs the spectra of the flat $(2\sqrt{3}\times\sqrt{3})R\,30^\circ$ monolayer (Figure 4, $a-c$) and the vicinal monolayer (Figure 4, $d-f$) it can be concluded that the step potential of the vicinal monolayer has a very strong influence on the formation of the monolayer electronic spectrum, especially along the $\overline{\text{X}\Gamma}$ direction perpendicular to the step. Here, the electronic bands radically change their dispersion $E(\mathbf{k})$ (become more flat) and shift in energy. A significant restructuring of the monolayer electronic spectrum is also observed in the $\overline{\Gamma\text{Y}}$ direction, which is almost parallel to the step. Almost all bands here experience splitting, but in general their dispersion, especially those marked by large orbital dichroism D_{xy}, maintains its tendency. It should be noted also that, as in the case of a flat monolayer, with an increase in the Bi atoms displacement on the terrace, the bands formed by its p_x- and p_y-states tend to lower binding energies (shift upward in energy), and the bands formed with the participation of its p_z-states tend to higher binding energies.

Comparing the electronic spectra of the Ag_2Bi surface alloy on thick films simulating the (1 1 1)-$(2\sqrt{3}\times\sqrt{3})R\,30^\circ$ smooth and the (4 2 3) vicinal surfaces (Figure 2, *c*), with the spectra of the smooth (Figure 4, *e*) and vicinal (Figure 4, *f*) Ag_2Bi hypothetical monolayer, it can be seen that the main spectral features of the surface alloy Ag_2Bi electronic structure, marked in Figure 2, *c* with the letters s_1, s_2 and s_3, turn out to be generally formed already at the monolayer level. However, in a monolayer, their energies are noticeably higher than in thick films.

Figure 5 shows the calculated electronic band spectra of the Ag_2Bi monolayers in the flat (1 1 1)-$(2\sqrt{3}\times\sqrt{3})R\,30^\circ$ (*a*) and vicinal (4 2 3) (*b, c*) configurations on the substrates of one (a, b) and three (c) silver layers. As follows from the figures, the addition of Ag substrate layers leads to a decrease in the contribution of the Bi p_z-states, instead of which the Ag atoms contribution increases. Although the Ag atoms contribution is not explicitly shown in the figure, it can be said to be present for those bands that lack any contribution from Bi states. Another main effect of adding a silver layer is to shift the bands down in energy. Thus, the addition of only one Ag layer (Figure 5, *a* and *b*) shifts the Bi states of the Ag_2Bi monolayer in such a way that they become very similar to the main spectral features of the electronic structure of

the Ag_2Bi surface alloy on thick films. The addition of three Ag monolayers (Figure 5, *c*) makes the spectrum of Bi states smoother and already reproduces the spectrum of the Ag_2Bi surface alloy quite well on thick films.

4. Conclusion

The genesis of the electronic states of the Ag_2Bi surface alloy on the Ag (4 2 3) vicinal surface is studied within the framework of the density functional theory. The change in the electronic structure of the Ag_2Bi surface alloy during the transition from the smooth surface of Ag (1 1 1)-$(\sqrt{3}\times\sqrt{3})R\,30°$ to the Ag (4 2 3) vicinal one was analyzed for this purpose. The role of surface vicinality, the role of silver substrate atoms and the relaxation of Bi atoms in the formation of the electronic spectrum of the Ag_2Bi surface alloy on the Ag (4 2 3) vicinal surface was studied within the framework of a model problem considering the Ag_2Bi hypothetical monolayer in the (1 1 1) flat and (4 2 3) vicinal (stepwise) configurations. It is revealed that the bands dispersion law of the Ag_2Bi surface alloy on a massive Ag (4 2 3) substrateis formed mainly due to the vicinal nature of the surface. The significant relaxation of the Bi atoms of the surface alloy causes the spin splitting of the energy bands and their displacement to lower binding energies. The atoms of the Ag substrate have little effect on the dispersion of the surface bands, but they significantly increase their binding energy. Even with the Ag substrate thickness of 3 atomic layers, the energy spectrum of the surface alloy does not fundamentally differ from the spectrum with the substrate thickness of 27 layers.

Thus, we have obtained a simple, intuitive model that sheds light on the origin of two-dimensional states and explains their dispersion observed in experiments using angular resolution photoemission spectroscopy.

Funding

The work was performed within the framework of the state assignment of the ISPMS SB RAS, topic No. FWRW-2026-0008, and with the financial support of Saint-Petersburg State University, project No. 125022702939-2.

Conflict of interest

The authors declare that they have no conflict of interest.

References

[1] C.R. Ast, J. Henk, A. Ernst, L. Moreschini, M.C. Falub, D. Pacilé, P. Bruno, K. Kern, M. Grioni. Phys. Rev. Lett. **98**, *18*, 186807 (2007).
[2] G. Bihlmayer, S. Blügel, E.V. Chulkov. Phys. Rev. B **75**, *19*, 195414 (2007).
[3] J. Premper, M. Trautmann, J. Henk, P. Bruno. Phys. Rev. B 76, 7, 073310 (2007).
[4] C.R. Ast, D. Pacilé, L. Moreschini, M.C. Falub, M. Papagno, K. Kern, M. Grioni, J. Henk, A. Ernst, S. Ostanin, P. Bruno. Phys. Rev. B **77**, *8*, 081407 (2008).
[5] I. Gierz, B. Stadtmüller, J. Vuorinen, M. Lindroos, F. Meier, J.H. Dil, K. Kern, C.R. Ast. Phys. Rev. B **81**, *24*, 245430 (2010).
[6] K.H.L. Zhang, I.M. McLeod, Y.H. Lu, V.R. Dhanak, A. Matilainen, M. Lahti, K. Pussi, R.G. Egdell, X.-S. Wang, A.T.S. Wee, W. Chen. Phys. Rev. B **83**, *23*, 235418 (2011).
[7] Sz. Vajna, E. Simon, A. Szilva, K. Palotas, B. Ujfalussy, L. Szunyogh. Phys. Rev. B **85**, *7*, 075404 (2012).
[8] S. Schirone, E.E. Krasovskii, G. Bihlmayer, R. Piquerel, P. Gambardella, A. Mugarza. Phys. Rev. Lett. **114**, *16*, 166801 (2015).
[9] C. Carbone, P. Moras, P.M. Sheverdyaeva, D. Pacilé, M. Papagno, L. Ferrari, D. Topwal, E. Vescovo, G. Bihlmayer, F. Freimuth, Y. Mokrousov, S. Blügel. Phys. Rev. B **93**, *12*, 125409 (2016).
[10] D. Go, J.-P. Hanke, P.M. Buhl, F. Freimuth, G. Bihlmayer, H.-W. Lee, Y. Mokrousov, S. Blügel. Sci. Rep. **7**, *1*, 46742 (2017).
[11] G. Bihlmayer, P. Noël, D.V. Vyalikh, E.V. Chulkov, A. Manchon. Nature Rev. Phys. **4**, *10*, 642 (2022).
[12] J.E. Ortega, G. Vasseur, F. Schiller, I. Piquero-Zulaica, A.P. Weber, J. Rault, M.A. Valbuena, S. Schirone, S. Matencio, L.A. Sviatkin, D.V. Terenteva, Y.M. Koroteev, E.V. Chulkov, A. Mugarza, J. Lobo-Checa. Phys. Rev. B **109**, *12*, 125427 (2024).
[13] P.E. Blöchl. Phys. Rev. B **50**, *24*, 17953 (1994).
[14] G. Kresse, J. Furthmüller. Phys. Rev. B **54**, *16*, 11169 (1996).
[15] G. Kresse, D. Joubert. Phys. Rev. B **59**, *3*, 1758 (1999).
[16] J.P. Perdew, K. Burke, M. Ernzerhof. Phys. Rev. Lett. **77**, *18*, 3865 (1996).
[17] D.D. Koelling, B.N. Harmon. J. Phys. C: Solid State Phys. **10**, *16*, 3107 (1977).
[18] Additional material for the study [12], at address http://link.aps.org/supplemental/10.1103/PhysRevB.109.125427

Translated by A.Akhtyamov